

EFFECT OF STATIC AND FATIGUE PRELOADING ON RESIDUAL STRENGTH AND STIFFNESS OF PLAIN CONCRETE

H.A.W. Cornelissen and H.W. Reinhardt*

The effect of compressive and tensile static as well as repeated tensile and alternating tensile-compressive fatigue preloadings on the reloading stress-strain relations in both compression and tension was experimentally investigated. For accurate control of the fatigue tests a newly developed system based on cyclic strain rate was applied. It was found that of all loading combinations, compressive preloading had a most detrimental influence on tensile reloading strength, but especially on reloading stiffness. These findings were explained on the basis of internal microcracking.

INTRODUCTION

For the assessment of the mechanical behaviour of structures and their constituent materials, the effect of loading history has to be taken into consideration. At any stage of service life a structure must be capable of sustaining the design loadings or deformations. Moreover information is needed about the ultimate capacity. However, it is well known that various types of preloading such as static, sustained and fatigue loadings affect the mechanical behaviour. Therefore these effects should be quantified and included in realistic computations in the design stage of a structure as well as after a certain service life in order to predict its remnant properties.

* Stevin Laboratory, Department of Civil Engineering, Delft University of Technology, The Netherlands.

SIGNIFICANCE OF THE RESEARCH

Up till now a lot of research work has been carried out for the investigation of fatigue behaviour of concrete under several loading conditions. Most research reflects constant amplitude tests which are commonly represented by S-N diagrams or summarized in a Smith or the Goodman diagram in Fig. 1 as proposed by Cornelissen and Siemes (1). Although more research is needed in this field, it can be seen in the figure that basic information is available for concrete loaded in tension (first quadrant), in compression (third quadrant) and in repeated tension-compression (second quadrant). Results from this type of constant amplitude tests can be translated to more complex loading conditions by the application of Miner's rule. Despite some fundamental shortcomings this rule is sufficiently accurate for practical prediction of service life. However, because the linear accumulation of damage on which Miner's rule is based, does not coincide with the real development of damage in the material, this rule only refers to an ultimate stage and not to intermediate changes of properties like strength and stiffness. Miner's rule in fact refers to the period of micro crack formation, after which a governing macro crack is initiated, which results in spontaneous failure because of stress concentrations in front of this crack. Especially the presence of such a macro crack is of importance for the remnant material properties.

Strength and stiffness behaviour as influenced by for instance fatigue preloadings were subject of various investigations. It turned out that for normal quality concrete loaded at normal rate, a fatigue compressive loading decreased compressive strength and stiffness significantly, while a compressive sustained load was slightly beneficial for these properties as shown by Cook and Chindaprasirt (2) and by Sri Ravindrarajah (3). These findings were explained by the effect of redistribution of stress concentrations in the cement paste in case of a sustained load, whereas a fatigue preloading produced limited microcracking.

Also by Cook and Chindaprasirt (4) and in (3) experiments are described in which a static tensile test was preceded by a sustained or fatigue loading in tension. Now both strength and stiffness were reduced.

Only a few results are available with respect to preloading followed by testing in the reversed direction. Tinec and Brühwiler (5) performed these types of tests from which it emerged that static as well as fatigue preloadings in compression prove to be detrimental for remnant tensile strength. No information on stiffness is known from these tests.

As pointed out before, knowledge on the effect of preloading is of importance for the assessment of remnant material properties. This can also be expressed in terms of fracture mechanics

application to concrete, which requires data on the complete stress deformation behaviour in tension as proposed by Hillerborg (6). Information is needed on Young's modulus (stiffness), tensile strength, shape of the descending branch and fracture energy G_f (see Figure 2). Assuming that G_f and shape of the descending branch remain unaffected by preceding loading, the influences on strength and stiffness provide sufficient data for the appropriate stress-deformation relation. The assumption stated, will be valid only if preloading does not affect crack opening relations.

In the present research project the effect of tensile as well as compressive preloadings on static strength and stiffness in uniaxial tension and compression are investigated. The preloadings consist of static loadings and various types of fatigue loadings.

EXPERIMENTAL DETAILS

Types of tests

Static load controlled uniaxial tests were performed after various preloading conditions which can be subdivided into two main types:

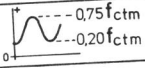
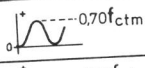
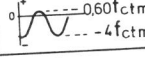
- static preloading

In these tests specimens were loaded up to 50% or 80% of the tensile strength or up to 50%, 80% or 90% of their compressive strength. The appropriate static strength values were estimated from tensile or compressive tests on similar specimens. The loading rate was always $0.1 \text{ N/mm}^2 \cdot \text{s}$.

- fatigue preloading

Constant amplitude tests were executed at a frequency of 6Hz. The tests comprised two groups with repeated tensile loadings, and one group with alternating tensile-compressive loadings. The tests were prolonged until a preset fraction of total number of cycles to failure was reached. These fractions denoted by cycle ratio n/N , were in the range of 20%-100%. An overview of the testing program is shown by table 1. It can be noted that the stress levels in the fatigue tests were chosen according to previous testing programs in which among others the relative damaging effect of tension-compression cycles was found. This effect can be observed in Figure 1 by the strong transition from the first to the second quadrant in the Goodman diagram.

TABLE 1 - Testing program for the fatigue preloading tests

type of test	cycle ratio n/N						
	0,20	0,50	0,75	0,85	0,90	0,95	1,0*
T1 		x	x	x	x	x	x
T2 	x	x	x	x	x	x	x
TC 	x	x	x	x	x	x	x

* up till failure

Specimen type and concrete composition

Specimens were drilled out of 200 mm cubes parallel to the casting direction. After that 25 mm was sawn from both ends, which resulted in specimens of 150 mm length. The specimens were tested at an age of 28 days. The curing conditions consisted of two weeks in water of 21°C followed by two weeks storage in the laboratory (about 21°C and 50% R.H.). Because of the maximum capacity of the testing machine, specimen diameter was chosen as 60 mm for the static preloading tests, whereas for the fatigue tests, with relatively low applied stresses, the diameter was 76 mm. Moreover in the latter case the specimens were provided with a circumferential saw cut (5 mm width and depth). Because of the distinct specimen diameters, concrete compositions were used with 16 mm maximum grain size for the fatigue preloading tests and with 8 mm for the static tests. An overview of both compositions, denoted by concrete A and concrete B, is shown in table 2. This table provides also information on density and 28 day standard control test results. For both concretes the splitting strength-compressive strength ratio proved to be 0.06, indicating comparable brittleness.

FRACTURE CONTROL OF ENGINEERING STRUCTURES – ECF 6

TABLE 2 - Mix proportions and standard mechanical properties

mix proportions	Concrete A static testing program (kg/m ³)	Concrete B fatigue testing program (kg/m ³)
Portland cement	375	325
sand 0-2 mm	905	565
sand 2-4 mm	363	312
gravel 4-8 mm	540	441
gravel 8-16 mm	-	623
water	187.5	162.5
density	2370	2415
mechanical properties	(N/mm ²)	(N/mm ²)
cube compressive strength	49.5 (3.2%)*	51.0 (1.9%)
splitting tensile strength	3.10 (4.1%)	2.87 (3.7%)

* coefficient of variation

Performance of the tests

The tests were carried out on a closed-loop electro hydraulic loading machine with static capacity of 150 kN both in tension and in compression. The specimens were glued between steel platens. The lower one was fixed, whereas the upper platen was connected to the actuator. Bending of the specimen was prevented by a guiding system provided with ball bushings of the upper platen. A schematic view of the loading arrangement is presented by Figure 3. It can be seen that the longitudinal deformation was measured with two LVDT's (base 65 mm) from which the averaged signal was monitored.

In order to control the loading, the signal from the load cell was compared with a signal from a function generator. With respect to this generator distinction has to be made between the static and the fatigue preloading tests.

Static tests. For these types of tests the loading signal was generated by a programmable signal generator, which made it possible to preset loading levels and loading rate (type: Feltron).

Fatigue tests. The control system for the fatigue preloading tests is schematically represented in Figure 3. Basically the cyclic loading signal was created by a generator which was controlled by a microcomputer. For the control system the known strong relation between secondary cyclic creep velocity ($\dot{\epsilon}_{sec}$) and number of cycles to failure (N) was applied (for clarification see figure in diagram 4). Previous research work in this field by Cornelissen (7) lead to the conclusion that an estimation of N was more accurate on the basis of $\dot{\epsilon}_{sec}$ than on the basis of applied stress-strength ratio. This is due to the fact that $\dot{\epsilon}_{sec}$ represents the actual loading state of the specimen, while in case of application of a given stress-strength ratio, this ratio is subjected to variations because of scatter in the strength.

The fatigue tests were started with loading cycles between preset maximum and minimum stress levels. From S-N lines measured before, N was estimated. Also $\dot{\epsilon}_{sec}$ was calculated from relations established in previous research (1,7). Reaching the secondary branch of the cyclic creep curve which was assumed to extend from 0.1N to 0.9N, $\dot{\epsilon}_{sec}$ was determined continuously from the measured deformation data. This measured $\dot{\epsilon}_{sec}$ was compared with the target value of $\dot{\epsilon}_{sec}$. Deviations were attributed to variations in actual concrete (tensile) strength, so both maximum and minimum stress levels were adjusted by the computer in such a manner that the preset stress-strength ratio's were realized. The ratio's chosen in the tests, resulted in number of cycles to failure from 10 to 50 thousand (T1: 30 000, T2:44 000, TC:12 000).

Using the procedure described, number of cycles to failure as well as fractions of it, could be predicted accurately. This is shown in Figure 4 in which test results are plotted from the three types of fatigue tests which were prolonged up till failure, meanwhile controlling the stress-strength ratio's by $\dot{\epsilon}_{sec}$. As can be seen the results are close to the predicted values as represented by the solid line in the diagram.

RESULTS

The results are represented in reloading stress-strain relations. Important features, like strength and stiffness, from these relations will be compared with results from virgin (not-preloaded) specimens. In table 3 averaged results for strength and stiffness from these virgin specimens are summarized. It is noted that in the table distinction was made between static and fatigue loading programs because of different mix composition (see table 2) and specimen diameter. Young's modulus was calculated as the secans value at 40% of the appropriate strength.

TABLE 3 - Mean strength and stiffness properties of not-preloaded specimens

property	Concrete A static testing program specimens $\phi 60$ mm (N/mm ²)	Concrete B fatigue testing program specimens $\phi 76$ mm (N/mm ²)
direct tensile strength	3.30 (9.3%)*	2.65 (4.9%)
Young's modulus (tension)	36160 (2.7%)	34400 (4.4%)
compressive strength	48.1 (6.9%)	
Young's modulus (compression)	31350 (3.0%)	

* coefficient of variation

In the following the results of static and fatigue preloading will be presented in succession.

Static preloadings

Specimens were preloaded in tension or in compression up to various stress-strength ratio's. These preloading conditions were combined with reloading either in tension or in compression. Typical stress-strain relations of tensile reloading tests are represented by Figure 5, whereas Figure 6 shows the corresponding curves for compressive reloading. Both figures include also individual curves from not-preloaded specimens. It can be observed in Figure 5 that tensile preloading has no influence on the curves. A compressive preloading (denoted by C1, C2 and C3), however, reduces stiffness significantly; there is no effect on tensile strength, but ultimate tensile strain increases from about 140 to 200 microstrain. These features are not observed in the compressive tests (see Figure 6). No significant deviations in strength, stiffness and ultimate strain were found here.

All strength and stiffness results are plotted in Figure 7 and 8 respectively. In these figures the results of preloaded specimens were referred to the averaged results of virgin specimens. It emerges from Figure 7 that only relatively high static compressive preloading (> 80%) reduces reloading tensile strength. In the diagram also some results from creep tests are indicated. These results are in accordance with the static test data. This is also valid for Young's modulus as represented in Figure 8. As mentioned before compressive preloading proves to be detrimental for reloading tensile stiffness.

Fatigue preloadings

Reloading tensile stress-strain curves were determined after three types of fatigue tests, which were interrupted at a preset fraction of number of cycles to failure. Sets of typical curves are represented for cycle ratio's being 0.50, 0.75 and 0.95 in Figures 9, 10 and 11 respectively. In these figures also the mean stress-strain relation of virgin specimens was drawn. It can be seen that especially stiffness is reduced and that mainly in the last stage of preloading ($n/N=0.95$) alternating tension-compression (TC) lowers tensile strength. An overview of strength and stiffness results is given by figures 12 and 13. Especially the effect of preloading on Young's modulus is evident. Even at 20% of total fatigue life, remnant stiffness is reduced by 20-40%. In case of tensile-compressive preloading this reduction reaches about 60%, close to failure. Repeated tensile fatigue loadings prove to be less damaging, but the reduction of stiffness still reaches 10-30%.

DISCUSSION

It emerged from the static preloading tests that an effect of tensile preloading on reloading tensile strength and stiffness could not be proved. This was also the case for a combination of compressive pre- and reloading. Compressive preloading, however, reduced reloading tensile stiffness significantly, while strength was reduced to less extent.

Fatigue preloading proved to be detrimental for Young's modulus especially in case of alternating tensile-compressive fatigue loadings. Tensile strength was only slightly affected by this type of preloading.

From all loading cases investigated, the combination compressive preloading and tensile reloading is most important. Obviously compressive damage caused by high static or prolonged fatigue pre-loadings, lowers tensile strength. Tensile stiffness, however, is reduced already by minor damage induced by compression.

The phenomena observed, can be understood by the fact that normal concrete properties are a result of cooperation of strong, stiff aggregate particles and the weaker matrix. By the action of a compressive load, longitudinal microcracks will be formed along the surfaces of the aggregate particles. This facilitates tensile deformation of the matrix, which results in a reduction of tensile stiffness (see Figure 14). At high induced compressive damage also ultimate tensile strain increases significantly for this reason. Tensile strength is basically influenced by transversal cracks, which will interact with longitudinal cracks only at an advanced stage of compressive damage when cracks which started in longitudinal direction along the grain surfaces curve away in

transversal direction.

CONCLUSIONS

1. Both static and fatigue tensile preloading ($< 0.8 f_{ctm}$) have minor influence on reloading strength and stiffness in tension or compression.
2. Reloading compressive strength and stiffness was found not to be affected by static compressive preloading ($< 0.8 f'_{cm}$).
3. Tensile strength and especially stiffness was strongly reduced by either static or fatigue compressive preloadings.
4. Accuracy of fatigue testing is improved by controlling secondary cyclic creep rate.
5. Further research is recommended to predict remaining life time of a structural component via nondestructive measurement of Young's modulus in tension.

ACKNOWLEDGEMENTS

The authors wish to thank CUR (Netherlands Centre for Civil Engineering, Research, Codes and Specifications) and MaTS (Marine Technological Research) for financial support. They also gratefully acknowledge the assistance received from ing. G. Timmers, ir. H. Voorsluis and mr. A.S. Elgersma.

REFERENCES

- (1) Cornelissen, H.A.W. and Siemes, A.J.M., Proceeding of the 4th Int. Conf. on Behaviour of Offshore Structures (BOSS'85) Elsevier Science Publishers b.v., 1985, pp. 487-498.
- (2) Cook, D.J. and Chindaprasirt, P., Magazine of Concrete Research, vol. 32, num.111, June 1980, pp. 89-100.
- (3) Sri Ravindrarajah, R., Int. J. of Cement Composites and Lightweight Concrete, vol. 4, num.4, Nov. 1982, pp. 251-252.
- (4) Cook, D.J. and Chindaprasirt, P., Magazine of Concrete Research, vol. 33, num.116, Sept. 1981, pp. 154-160.
- (5) Tinec, C. and Brühwiler, E., Int. J. of Cement Composites and Lightweight Concrete, vol. 7, num.2, May 1985, pp. 103-108.
- (6) Hillerborg, A., "Fracture mechanics of concrete", Ed. F.H. Wittmann, Elsevier Science Publishers, Amsterdam, 1983, pp. 223-249.

- (7) Cornelissen, H.A.W., Proceeding 5th European Conference Fracture, Lisbon, 1984, pp. 729-738.
- (8) Fouré, B., Ann. de l'Inst. Techn. du Batiment et des Travaux Publics, no. 432, 1985, pp. 1-15.

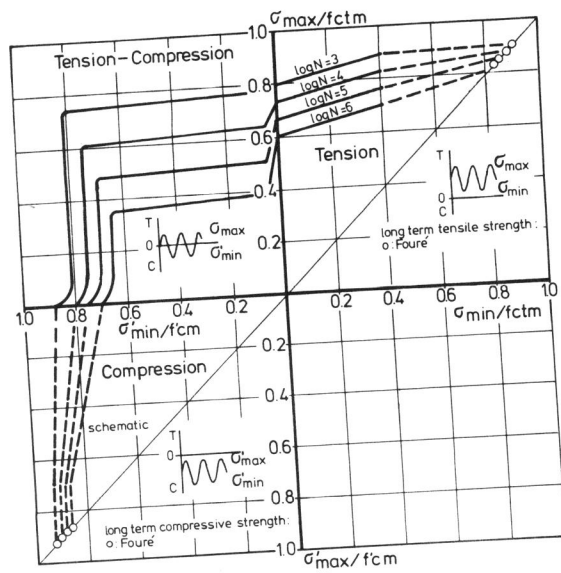


Figure 1 Modified Goodman diagram for dry concrete tested at 6Hz (long-term strength properties were taken from Fouré (8))

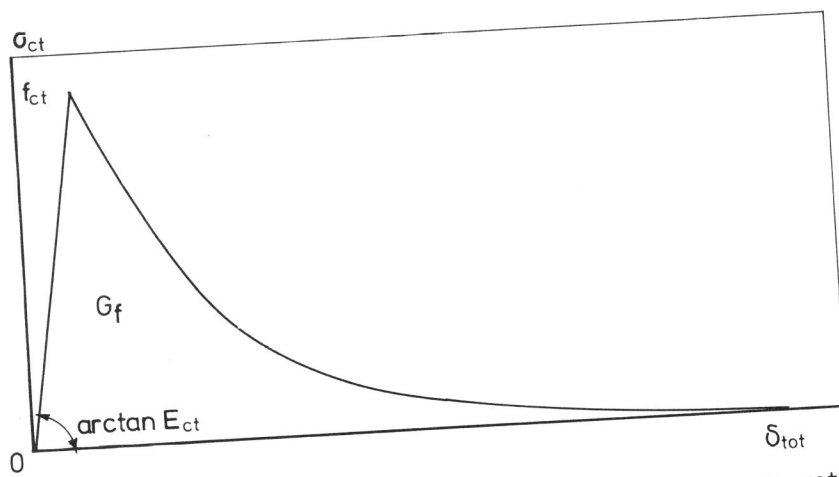


Figure 2 Schematic total stress-deformation relation for concrete in tension.

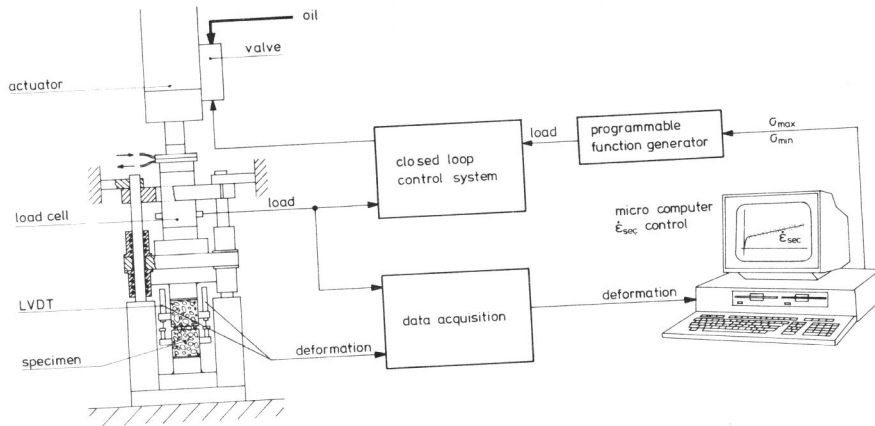


Figure 3 View of the testing equipment completed with the control system for the fatigue tests.

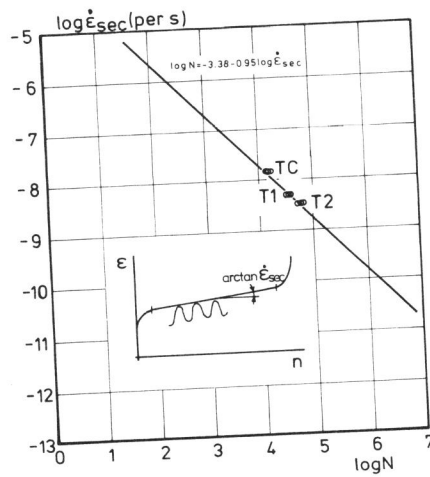


Figure 4 Predicted and measured number of cycles to failure by $\dot{\epsilon}_{sec}$ control (see table 1 for notation).

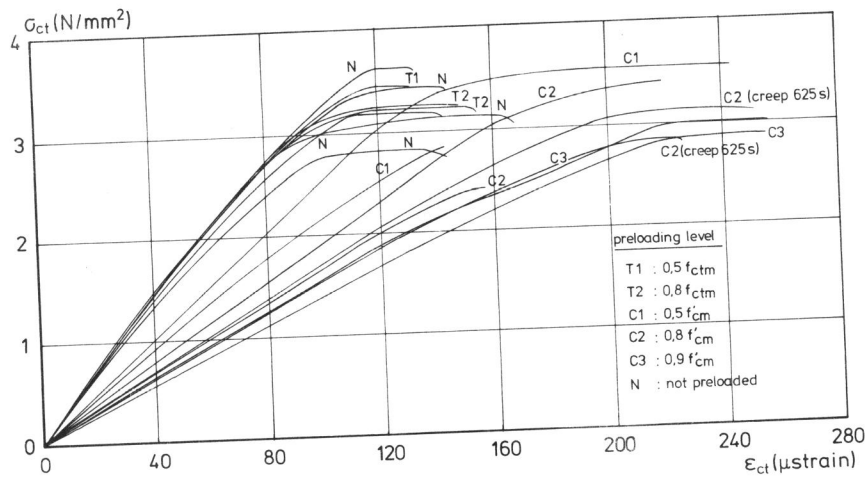


Figure 5 Tensile stress-strain curves after the indicated types of static preloadings.

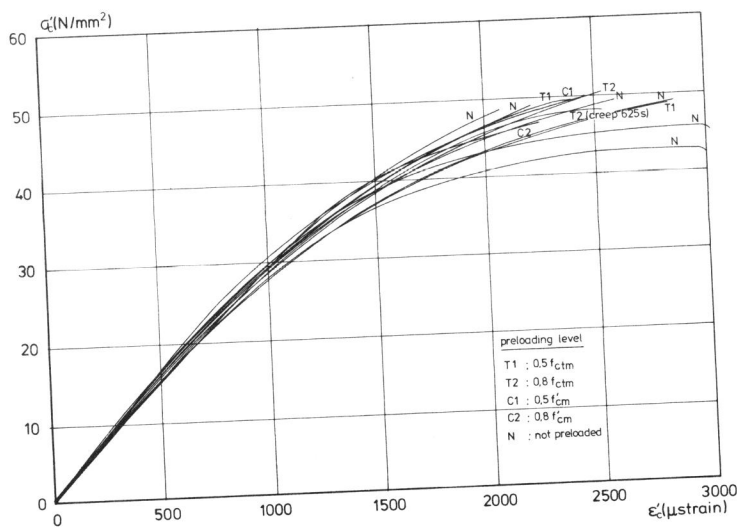


Figure 6 Compressive stress-strain curves after the indicated types of static preloadings.

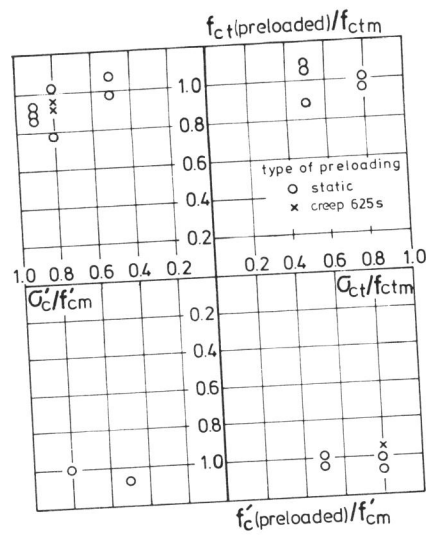


Figure 7 Effect of static preloading on relative strength.

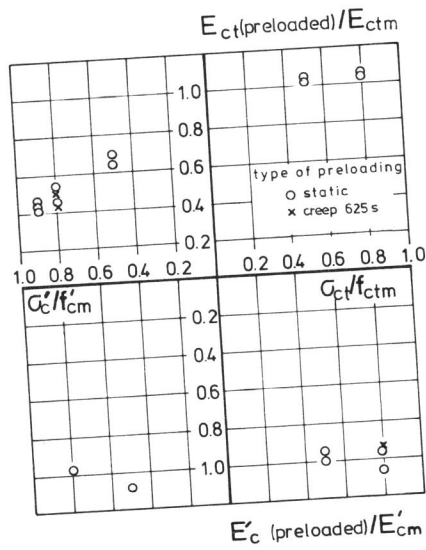


Figure 8 Effect of static preloading on relative stiffness.

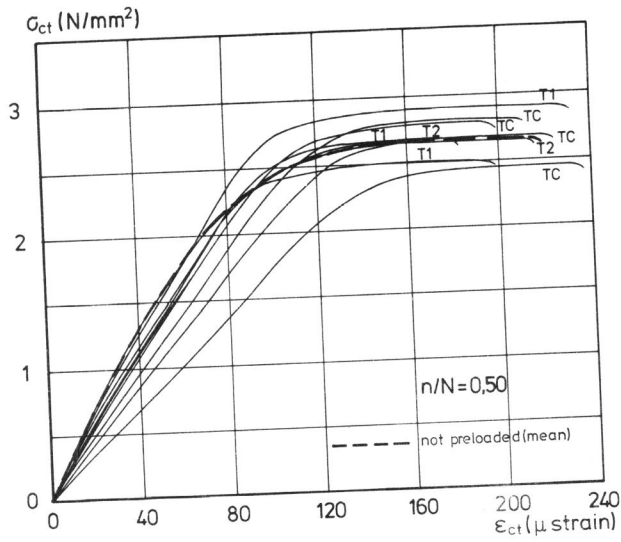


Figure 9 Tensile stress-strain curves after fatigue preloading up to a cycle ratio of 50% (for notation see table 1).

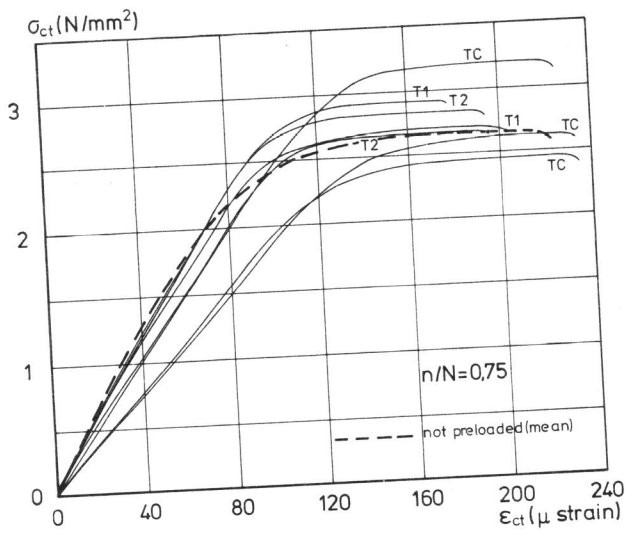


Figure 10 Tensile stress-strain curves after fatigue preloading up to a cycle ratio of 75% (for notation see table 1).

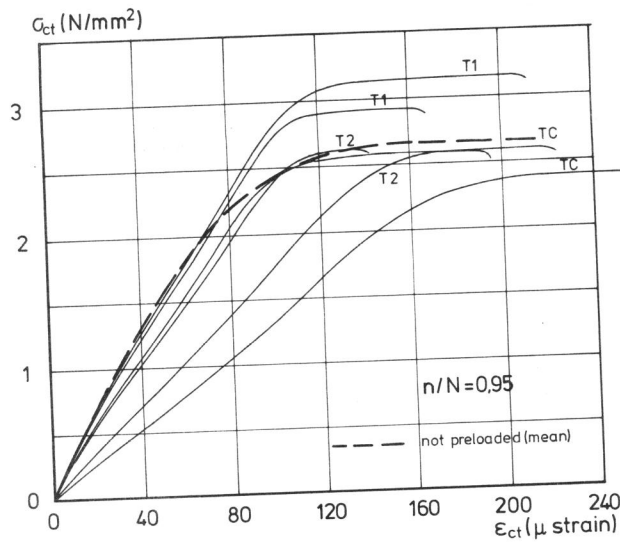


Figure 11 Tensile stress-strain curves after fatigue preloading up to a cycle ratio of 95% (for notation see table 1).

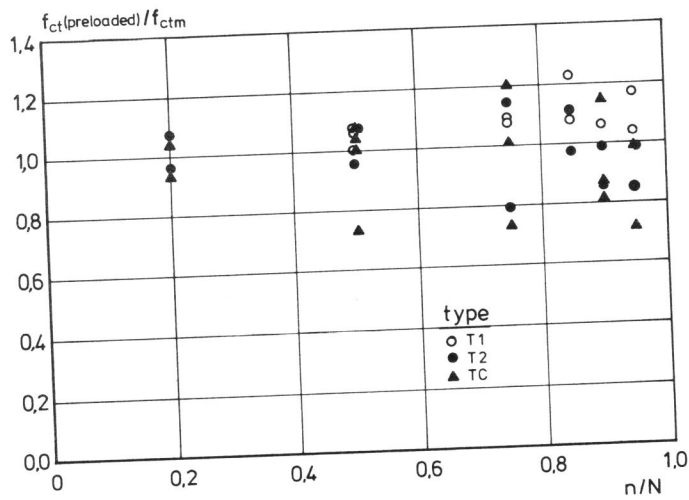


Figure 12 Static tensile strength as influenced by fatigue preloading (for notation see table 1)

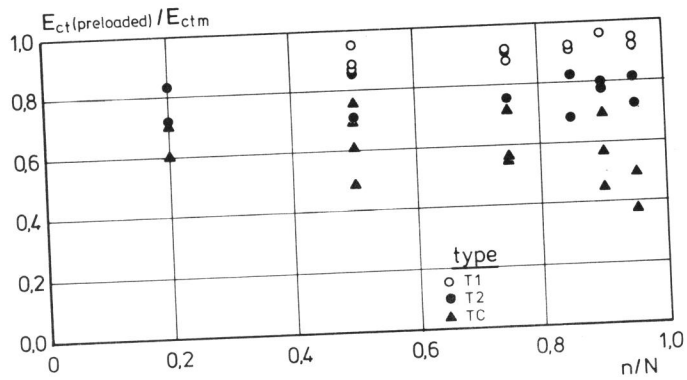


Figure 13 Static tensile stiffness as influenced by fatigue preloading (for notation see table 1)

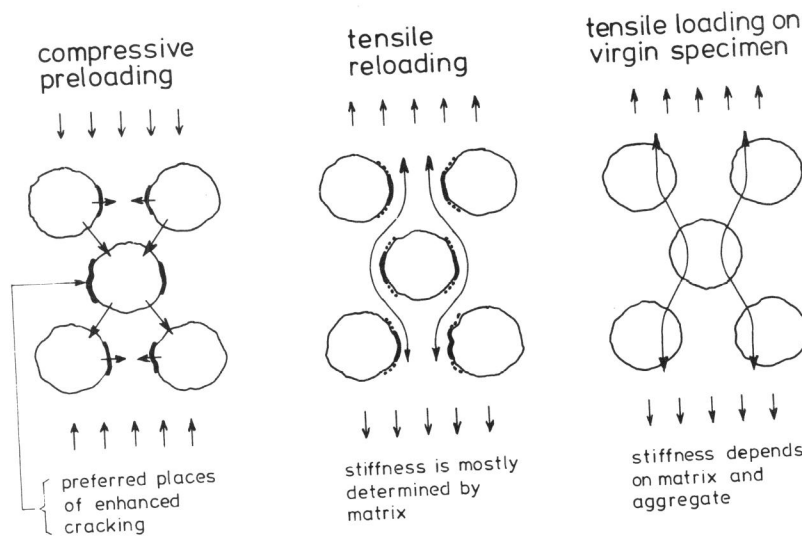


Figure 14 The effect of microcracking induced by compression on reloading tensile properties.